Am J Transl Res 2021;13(12):13697-13709
www.ajtr.org /ISSN:1943-8141/AJTR0133028

Original Article

Multi-omics-based identification of atopic dermatitis target genes and their potential associations with metabolites and miRNAs

Animesh Acharjee[1,2,3], Elizaveta Gribaleva[4], Subia Bano[5], Georgios V Gkoutos[1,2,3,6,7,8]

[1]College of Medical and Dental Sciences, Institute of Cancer and Genomic Sciences, University of Birmingham, Edgbaston, Birmingham B15 2TT, UK; [2]Institute of Translational Medicine, University Hospitals Birmingham NHS, Foundation Trust, Edgbaston, Birmingham B15 2TT, UK; [3]NIHR Surgical Reconstruction and Microbiology Research Centre, University Hospital Birmingham, Birmingham B15 2WB, UK; [4]Department of Dermatology and Venereology, I.M. Sechenov First Moscow State Medical University (Sechenov University), Moscow 119435, Russian Federation; [5]Elvesys Microfluidic Innovation Centre, Paris 75011, France; [6]MRC Health Data Research UK (HDR UK), Midlands Site, Birmingham B15 2TT, UK; [7]NIHR Experimental Cancer Medicine Centre, Birmingham B15 2TT, UK; [8]NIHR Biomedical Research Centre, University Hospital Birmingham, Birmingham B15 2TT, UK

Received March 11, 2021; Accepted August 16, 2021; Epub December 15, 2021; Published December 30, 2021

Abstract: Atopic dermatitis (AD), or atopic eczema, is one of the most common inflammatory skin diseases with up to 10% prevalence in adults, and approximately 15-20% in children in industrialized countries. As a result, there is an unmet need for faster, safer, and effective treatments for AD. AD pathogenesis represents a complex interplay between multiple factors, such as environmental factors or stimuli, genetic factors, immune dysfunctions. However, although multi-omics label studies have been very useful in understanding the pathophysiological mechanisms of AD and its clinical manifestations, there have been very few studies that integrate different labels of omics data. Here, we attempted to integrate gene expression and metabolomics datasets from multiple different publicly available AD cohort datasets and conduct an integrated systems-level AD analysis. We used four different GEO transcriptome data sets and, by applying an elastic net machine learning algorithm, identified robust hub genes that can be used as signatures, for example, H2AFX, MCM7, ESR1 and SF3A2. Moreover, we investigated potential associations of those genes by applying a pathway-based approach over metabolomics and miRNA datasets. Our results revealed potential novel associations between fatty acids and peroxisomal lipid metabolism pathways, as well as with several microRNAs.

Keywords: Multi-omics, machine learning, atopic dermatitis (AD), eczema, pathway analysis, translational research

Introduction

Atopic dermatitis (AD) is one of the most common inflammatory skin diseases with around 10% prevalence in adults, and approximately 20% in children [1]. AD is typically considered the result of a complex interplay between multiple factors, such as environmental factors or stimuli, genetic factors [2], immune dysfunctions, and host-microbiome interactions [3]. Omics analysis has been widely used in recent years to explore potential biomarkers and to gain a better understanding of the underlying pathobiology and pathophysiology of various clinical forms and different disease subtypes [3]. Numerous studies have been carried out in an effort to cater the molecular AD diagnosis, many of which entailing the analyses of high throughput omics experiments, namely transcriptomics [4-6], metabolomics [7, 8], proteomics [9, 10], etc. The primary objective of such studies is to identify markers that can be targeted for drug discovery or be used for the identification of biomarkers that cater disease stratification [11]. Although single-omics studies have been very useful for understanding the AD mechanisms and manifestation, multi-omics approaches offer the tantalising possibility of gaining an in-depth understanding of AD's complex pathogenesis [3]. Currently, very few stud-

Table 1. GEO datasets employed in this study

GEO ID and reference	Data types	Platform used	Sample size	Tissue type
GSE36842 [20]	Microarray	GPL570, Affymetrix Human Genome U133 Plus 2.0 Array	Normal = 15, AD = 8, Total = 23	Skin Biopsies
GSE16161 [21]	Microarray	GPL570, Affymetrix Human Genome U133 Plus 2.0 Array	Normal = 9, AD = 9, Total = 18	Skin Biopsies
GSE6012 [22]	Microarray	GPL96, Affymetrix Human Genome U133A Array	Normal = 10, AD = 10, Total = 20	Skin Biopsies
GSE32924 [23]	Microarray	GPL570, Affymetrix Human Genome U133 Plus 2.0 Array	Normal = 10, AD = 10, Total = 20	Skin Biopsies
ST001431-Metabolomics workbench [66]	Metabolomics	LC-MS targeted	Normal = 24, AD = 25, Total = 49	Blood Serum

ies integrating different omics labels have been conducted [3]. Several studies examined the integration of lipidomics and transcriptomics [12], or transcriptomic and proteomic data [13], as well as of epigenetic and transcriptomic datasets [14] to explore the microenvironment and immune regulation in AD skin. Moreover, one recent study investigated the association of the infant gut microbiome with its metabolome in order to understand the impact of the microbiome on the risk of AD development [15]. While single omics approaches appear to be insufficient in identifying biomarkers for AD endotyping, novel multi-omics integration methods offer the potential of gaining a better understanding of the underlying AD molecular patterns, as well as of a potential interpretation of AD clinical variability [3].

In the present study, we attempted to integrate gene expression, miRNA and metabolomics datasets from multiple cohorts, and obtain an integrated systems-level overview of AD. Four different GEO transcriptome datasets were used and robust gene signatures determining core AD pathogenetic elements were identified. Furthermore, by adopting pathway-based approaches, it was demonstrated that metabolomics signatures were associated with particular gene signatures revealing novel genes, metabolites, and miRNAs associations.

Methods

Data collection

Table 1 lists the gene expression datasets obtained from the Gene Expression Omnibus (GEO) [16], as well as the metabolomics dataset retrieved from the MetabolomicsWorkbench [17]. All datasets were collected on 30th November 2020.

Differential expression analysis using GEO2R

We used the GEO2R [18], an online tool employing the limma package [19], to identify differential genes (DEGs) between normal vs. AD skin. For this analysis, two groups were created (normal vs. AD) for each individual dataset using the GEO 'define groups' feature. Genes without a corresponding gene symbol and genes with more than one probe set were removed. The statistical significance values were set as adjusted *P*-value ≤0.05. Three GEO series datasets were used, namely GSE36842 [20], GSE16161 [21], and GSE6012 [22], to identify differential expressed genes, and the GSE32924 dataset [23] was used for validation. An overview of the workflow (process) is presented in **Figure 1**.

Differentially expressed genes networks

A network analysis of the selected differentially expressed genes (DEGs) was subsequently performed using the OmicsNet tool [24]. Using this tool, we mapped protein-protein interactions and transcription factor-gene interactions. Protein-protein interactions were mapped using a manually curated experimentally validated PPI database (IntAct). Moreover, the number of connections (node interactions) for each of the differentially expressed genes was calculated, and only genes with more than 100 interactions were considered for further analysis.

Gene marker selection using machine learning methods

We applied two feature selection methods, namely the Least Absolute Shrinkage and Selection Operator (LASSO) [25] and the Elastic Net (EN) [26] methods. Both EN and LASSO are able to automatically select the best features

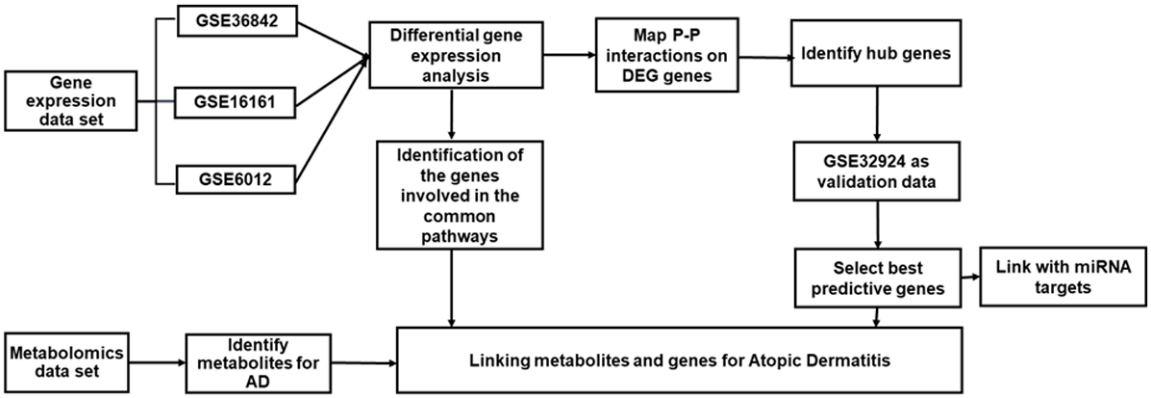

Figure 1. Overview of the study workflow and methods.

linked with an outcome variable (for example, normal vs. AD). Both EN and LASSO are considered penalty-based methods and hence provide a sparse solution. The penalty parameter, λ (range of λ: 0-1), was optimized using 10-fold cross-validation. For the case of LASSO, the penalty is applied to the sum of the absolute values of the regression coefficients (L1 norm). Elastic Net, on the other hand, employs a mixed version of both L1 and L2 penalty (Ridge penalty). We combined selected variables identified by both LASSO and EN and then applied a generalized linear model (GLM) to cater for the stability analysis of the selected features. The process was repeated 100 times and the features were ranked according to their respective selection frequency associated with each run. We then selected the first quartile of the combined LASSO and EN selected features over 100 runs. These selected features were then further modelled using logistic regression. Two area under the curve (AUC) distributions resulted from this analysis. The one related to random label sampling (i.e., the randomization of sample labels in each iteration, averaged over 100 iterations) was termed as 'random AUC'. The second distribution was based on the bootstrapped samples.

Enrichment analysis and miRNA association analysis

The enrichment analysis of identified DEGs was then performed to assess the potential molecular pathways, gene functions or biological processes associations. Pathway analysis was subsequently performed over the differentially expressed genes using the OmicsNet tool [24] and the KEGG gene database. Pathways of interest were subsequently inspected to identify DEGs. The metabolomic enrichment analysis was performed using the IMPaLA (Integrated Molecular Pathway-Level Analysis) [27] web tool. We merged miRNA information with the genes selected from the previous step using the NetworkAnalyst v3.0 webtool [28].

Statistical analysis

R version 4.0.3 [29] was used for statistical analyses. For differential expressed genes between normal vs AD skin samples, Benjamini-Hochberg (BH) adjusted *P*-value ≤0.05 was considered. Metabolites were analysed using a Wilcoxon rank test and *P*-values of <0.05 were considered statistically significant.

Results

Hub genes identification

Publicly available GEO datasets were used to identify genes that are differentially expressed between AD vs. control samples. We mapped protein-protein interactions (PPI) using a validated PPI database (IntAct) [30] that allowed us to identify highly connected genes (called degree). Within the GSE36842 dataset, we identified the GABARAPL1 gene to have the highest degree with 519 connections. In total, 10 genes were selected with a degree of more than 100 from the GSE36842 dataset. For the GSE6012 dataset, we found 24 genes with a degree more than 100 that were considered hub genes. The MYC gene was found to have the highest degree with 769 connections. Similarly, for the GSE16161 dataset, GRB2 was identified to have the highest number of the

Table 2. Hub genes and predictive genes

GEO-ID	Hub genes (>100 P-P connectivity)	Elastic Net predictive genes
GSE36842	10	10
GSE16161	9	7
GSE6012	24	6

degree, and in total nine genes were identified. No common genes shared across three datasets were found. One common gene, namely CALM3, was identified between the GSE36842 and GSE6012 datasets and one common gene, YWHAZ, was found between GSE6012 and GSE16161 datasets. The list of the genes and their corresponding degrees is presented in Supplementary Table 1.

Elastic net-based selection of predictive genes

We applied the EN method using the identified hub genes from each of the datasets separately to select the important discriminating genes between AD and control samples. From GSE36842, EN selected 10 genes out of 10 input hub genes. From GSE16161, EN selected seven genes out of nine input hub genes and finally from GSE6012, EN selected six genes out of 24 hub input genes (**Table 2**). To investigate the predictive performance of the identified genes, we used an external validation dataset, GSE3292. Nine genes were identified within the validation dataset and a logistic regression model was applied to obtain their individual as well as combined predictive power between control vs. AD samples. The individual AUCs for each of the genes with confidence interval (CI) were found: H2AFX (AUC: 1.000, CI: 1-1), MCM7 (1.000, CI: 1-1), ESR1 (0.971, CI: 0.88-1), SF3A2 (0.846, CI: 0.64-0.98), UBA1 (0.601, CI: 0.21-0.63), TP53 (0.577, CI: 0.37-0.81), EF1A1 (0.572, CI: 0.36-0.76), GIGYF2 (0.567, CI: 0.38-0.78), PPP2CA (0.510, CI: 0.23-0.75). Out of these genes, four, namely, H2AFX, MCM7, ESR1, SF3A2, were associated with regression models with AUC values higher than 0.80. **Figure 2A** depicts box plots of the predicted genes with associated *P*-values, while **Figure 2B** presents the AUC values of the combined regression model.

Gene set enrichment analysis

A pathway and gene enrichment analysis was performed to identify potential pathway associations. The top five pathways identified were the Class I PI3K signaling events, the integrin family cell surface interactions, the Arf6 trafficking events, endothelins, the EGF receptor (ErbB1) signalling, as well as IL-3-, IL-5- IL-8- and IFN-gamma-related immune signalling pathways. Multiple genes were found to be associated with those pathways (**Figure 3**). A list of these genes and their associated pathways is provided in Supplementary Table 2. We further investigated genes involved in biological processes such as cell cycle regulation, apoptosis, signal transduction, DNA replication, immune response, etc (**Figure 3**).

miRNAs associations

NetworkAnalyst was then used to explore potential miRNA associations with the previously identified genes. The TP53 gene was identified as having the highest numbers of interactions (also called as degree) amongst them, interacting with 130 miRNAs. The degrees of the PPP2CA, ESR1, EEF1A1, and MCM7 genes were 68, 90, 61 and 90, respectively. **Figure 4A** provides a visualisation of the predictive genes and their associations with miRNAs. The miRNA-gene interacting pairs are reported in Supplementary Table 3.

Metabolite identification

A Wilcoxon rank test obtaining *P*-values ($P < 0.05$) was performed over the serum metabolomics dataset (ID number ST001431). Cetylcarnitine, phosphatidylcholine diacyl, phosphatidylcholine diacyl, acylcarnitines, carnitine, acetylcarnitine, dicarboxylacylcarnitines were found to be significant. For these metabolites, a metabolic enrichment analysis was also conducted using IMPaLA. The top three metabolic pathways identified were the beta-oxidation of pristanoyl-CoA, peroxisomal lipid metabolism, and fatty acid metabolism pathways, while acetylcarnitine, phosphatidylcholine diacyl, carnitine and acylcarnitines were associated with those pathways significantly. A bar graph of the pathways identified and their associated (-log10) *P*-values are presented in **Figure 4B**.

Discussion

In this study, we aimed to identify candidate genes relevant to AD and to associate them with particular metabolites and miRNAs. We identified H2AFX, MCM7, ESR1, SF3A2, UBA1,

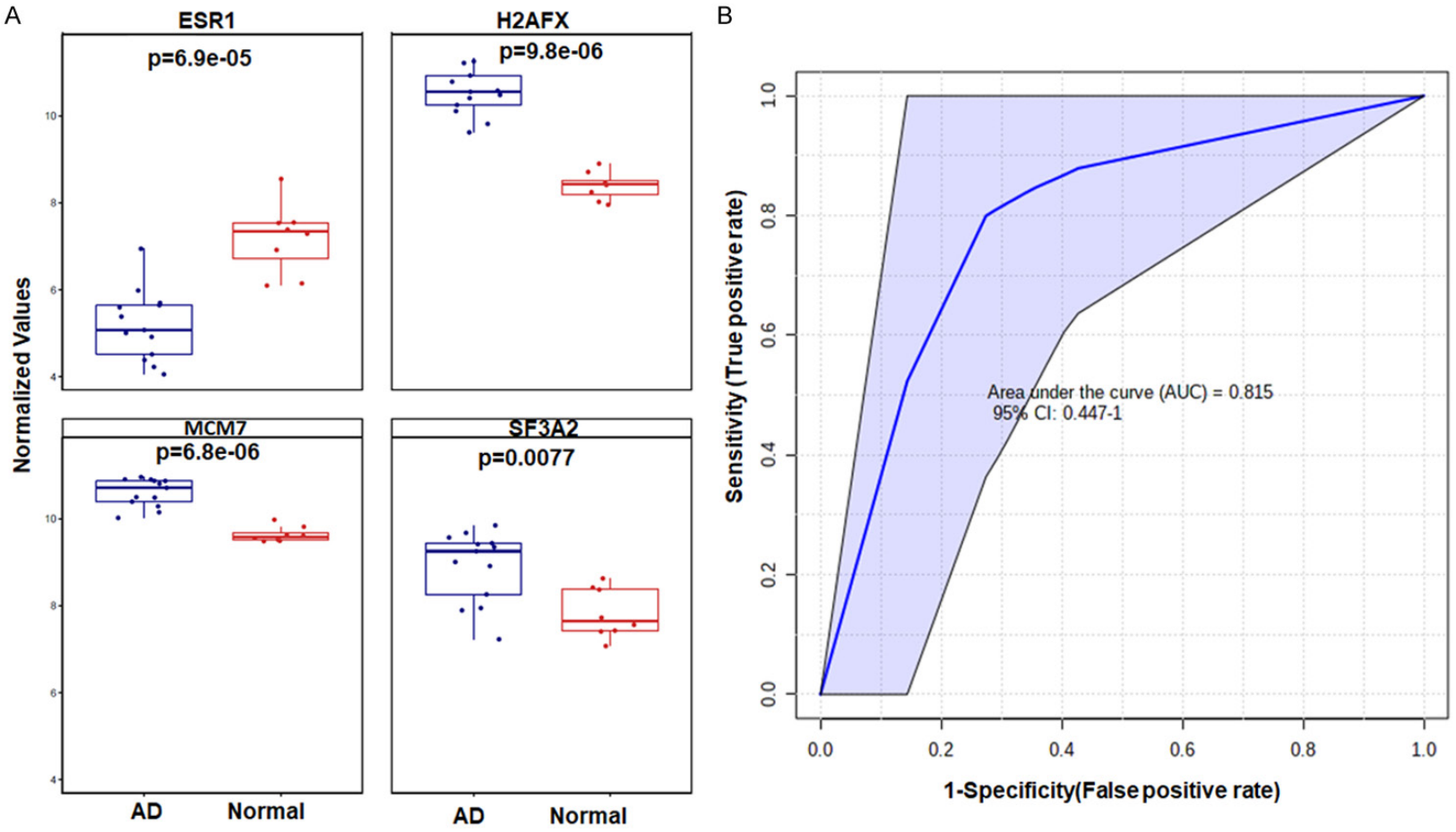

Figure 2. A. Box plots of the predictive genes across AD vs. control samples. Significant (P<0.05) gene up-regulation is represented in solid red for the healthy patients and gene down-regulation is highlighted in solid blue for the AD patients. B. An AUROC with 0.81 value and a CI (0.44-1) related to the performance of the model using 4 genes on the GSE32924 dataset.

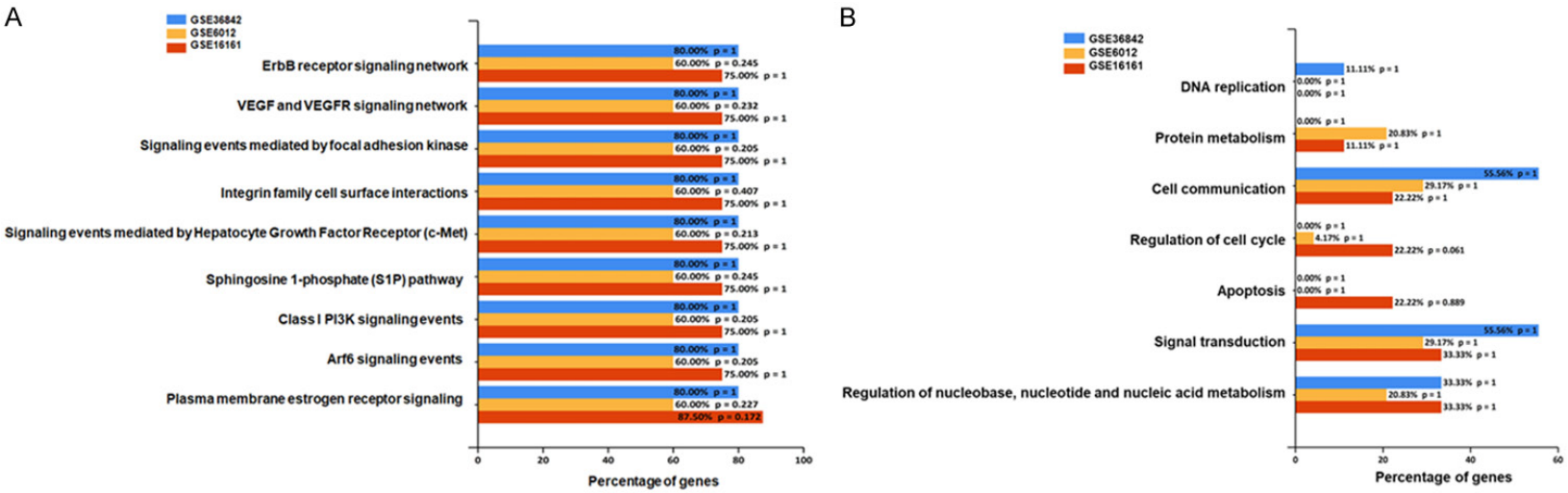

Figure 3. (A) Common pathways identified across multiple GEO data sets and (B) common biological processes identified across multiple GEO data sets.

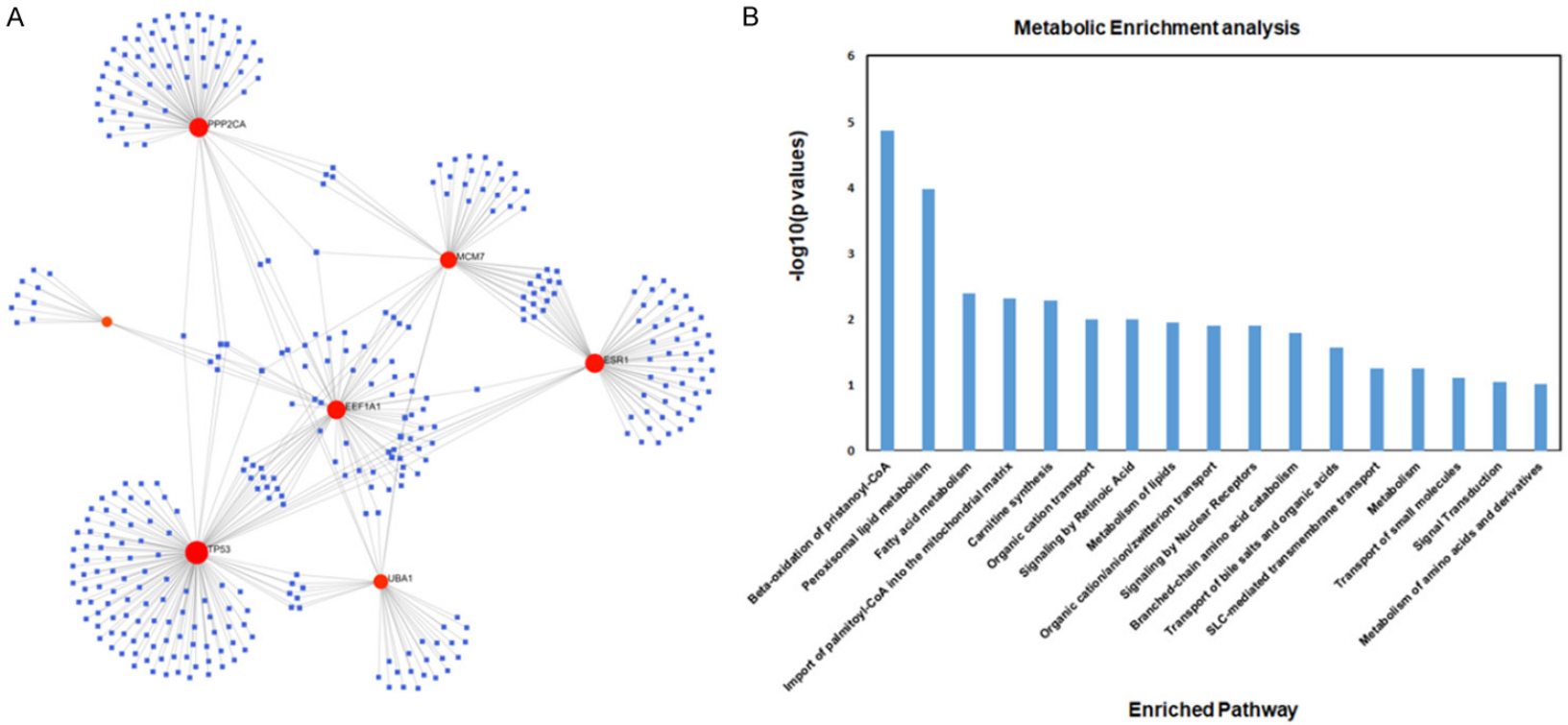

Figure 4. A. Selected predictive genes with miRNA targets associations. B. Metabolite enrichment analysis using IMPaLA. The figure depicts the pathways found to be associated with AD (X-axis) and their associated-log10 (*p*) values (Y-axis).

TP53, EEF1A1, GIGYF2, PPP2CA as the hub and predictive genes. H2AFX is an H2A histone family member contributing to the chromatin-remodeling and the nucleosome-formation DNA repair preserving genetic integrity. H2AFX mutations have been shown to lead to breast cancer [31]. H2AFX has also been implicated in the hypoxia-driven neovascularization process [32]. The minichromosome maintenance complex (MCM) is known to be involved in pre-replication complex formation that helps in DNA denaturation and unwinds the replication fork [33]. The MCM complex is composed of six highly conserved MCM proteins [34, 35]. Most of the MCM proteins are involved in carcinogenesis. Among them, MCM7 is considered to be an important unit of heteromeric MCM helicases which play a key role in controlling DNA replication and cell proliferation. A high level of MCM7 gene expression is also associated with tumour progression and metastasis and is considered an important cancer biomarker [36]. MCM7 has also been reported to be associated with hepatic carcinogenesis, esophageal squamous cell carcinoma, and prostate carcinoma [33, 37, 38]. Furthermore, MCM3 and MCM7 were demonstrated to be differentially expressed in primary T-cell cutaneous lymphoma skin samples [39]. MCM7 was also demonstrated to have higher levels of expression in skin proliferative disorders, such as keratoacanthoma, verruca vulgaris, and psoriasis vulgaris in comparison with normal skin [40]. ESR encodes estrogen receptor-alpha (ER-α), which is one of the potential targets in breast cancer treatment. It acts as a transcriptional regulator by interacting with estrogen and other proteins and has a role in breast cancer progression. ESR1 genetic variants are known contributors to breast carcinogenesis by inducing cell proliferation, genetic mutation, and necrosis [41]. The ESR-1 gene, encoding ESR-α, has been used as a target in therapy for breast cancer. Several miRNAs (miR-22, miR 301a-3p, miR 206) were reported to suppress the expression of ER-α via direct binding with the 3'UTR (untranslated region) of ESR1 mRNA, which provided resistance to estrogen/ERα-targeted therapies [42, 43]. Gao et al. have shown that expression of the ESR1 gene was regulated through a miRNA-mRNA regulatory pathway in ERα positive breast cancer [43]. They validated their results through a series of in silico studies and experimental analysis. Based on these findings, it was concluded that the miRNA targeted therapy emerged as a promising strategy for breast carcinoma. Moreover, the ERS1 gene has been shown to be differentially expressed in psoriasis, a chronic cutaneous inflammatory condition driven by IL-17 and IL-12/23 immune dysregulation [44]. As for SF3A2, a genome-wide screening in Drosophila and human cells showed the RNAi-mediated depletion of many different splicing factors (SF) to be associated with mitotic defects, ranging from abnormal chromosomal segregation to cytokinesis failure. SF are also involved in the mitotic division by disrupting the nuclear envelope. Pellacani et al. explored the role of SF3A2 in mitosis in Drosophila and humans reporting that the SF depletion influences the spindle formation and disrupts chromosomal segregation [45]. PPP2-CA, protein phosphatase 2 catalytic subunit alpha gene, negatively controls cell growth and division. Also, in the study of Fang et al., it was proposed that PPP2CA played an important role in epidermis and hair follicles development in mice [46].

The gene enrichment analysis showed that ESR1, TP53, and PPP2CA were linked with integrin family cell surface interaction, endothelins, and immune pathways of IL-3- IL-5-, and IL-8 mediated signaling. IL-3 is a multi-lineage colony-stimulating factor produced by lymphoid cells and eosinophils [47]. IL-5 is an eosinophil colony-stimulating factor activating eosinophils, while IL-8 is one of the proinflammatory chemokines [48]. Moreover, Ghosh et al. also proposed that integrin-linked kinase (ILK) signaling and endothelin signaling were involved in the pathogenesis of AD [3]. While ILK activation may be connected with S. aureus colonization of AD skin, endothelin-1 plays a role in mediating itch, one of the most prominent symptoms of AD [3].

Our gene enrichment analysis also depicted an association of MCM7 and PPP2CA with the TNF alpha/NF-κB signaling pathway. NF-κB is a crucial effector molecule of inflammation and was proven to be involved in AD immune pathologic signaling [49].

Genome-wide association studies (GWAS) have revealed the association of FLG and KIF3A with atopic dermatitis, resulting in a disrupted skin barrier and reduced clearance of allergens, respectively [3]. Moreover, the meta-analysis

of AD-derived transcriptome datasets highlighted the importance of inflammatory markers (MMP12) as well as the genes involved in T-cell immunity activation (Th2/CCL18, Th1/IFN/CXCL10, Th17/PI3/elafin, Th17/Th22 S100A7/A8/A9), epidermal proliferation (KRT16, Mki67, CLDN8), markers of atherosclerosis signalling (IL-37, selectin E), and downregulation of epidermal lipids (FA2H, FAR2, ELOVL3) [50]. Ghosh et al. analysed five publicly available AD transcriptome datasets and used clustering analysis to identify the genes that were differentially expressed in AD skin [51]. They performed validation experiments over the findings and demonstrated that genes involved in the epidermal barrier function, inflammation-related genes, proteases and protease inhibitor genes, as well as genes of antimicrobial responses, were differentially expressed in AD [51]. Our predictive genes are different from the ones previously identified. This might be due to the different datasets and samples used, and potentially due to our study focus on the identification of the genes involved in multiple interactions with proteins and miRNAs.

Several studies have been conducted exploring the miRNAs involved in AD pathogenesis. MicroRNAs are non-coding RNA molecules involved in post-transcriptional changes, which can negatively modify gene expression by degrading mRNAs or lowering their quantity [52]. Dysregulation of miR-143, miR-146a, miR-151a, miR-155 and miR-223 has been reported in AD patients [53]. These miRNAs play a role in the regulation of proliferation and apoptosis of keratinocytes, immune signalling (e.g. cytokine and nuclear factor-κB-dependent inflammatory responses), as well as the activity of Th-17 and Treg cells [53]. Moreover, the analysis of child AD datasets revealed miR-451 to be a potential predictive biomarker for early diagnostics [54]. Nousbeck et al. reported that miRNA-451a targets the interleukin 6 receptor (IL6R) and the proteasome subunit beta type-8 (PSMB8), while IL6R and PSMB8 showed a negative correlation with miR-451a levels in peripheral blood mononuclear cells (PBMCs) [54]. Furthermore, miRNA-155 expression was found to correlate positively with the severity of AD, Th-17 cell percentage, IL-17 mRNA expression and its plasma concentration [55]. In our study, we identified mir-155-3p, mir-151a-5p and mir-223-3p to be associated with p53 gene expression; these miRNAs were reported to play a role in the regulation of immune pathways in AD [53].

Tonacci et al. reviewed the role of different microRNAs in AD and ASD (Autism Spectrum Disorder) patients [56]. They reported that the main dysregulated miRNAs in AD are miR-186, miR-361-3p, miR-605, mir-150, mir-455-3p, and mir-302c-3p. Out of these miRNAs, our analysis identified miR-361-3p and mir-455-3p to be interacting with FFF1A1, mir-605 to be interacting with TP53, and mir-302c-3p to be interacting with MCM7.

From the metabolomic analysis conducted, we identified phosphatidylcholine diacyl, carnitine, acetylcarnitine and acylcarnitines to have either higher or lower abundance in AD patients. Those metabolites are associated with beta-oxidation of pristanoyl-CoA, peroxisomal lipid metabolism, and fatty acid metabolism pathways, which are essential for energy metabolism [57, 58]. It is known that epidermis exhibits extensive levels of lipid metabolism to maintain the barrier function [59]. Furthermore, peroxisomes play a role in the proliferation, differentiation of cells as well as in the modulation of inflammatory responses [60]. Few metabolomic studies have been conducted in the context of AD. In the study by Huang et al. [61], which was focused on the metabolome of children with AD, it was reported that tryptophan and indolelactic acid (tryptophan metabolism pathway members), taurochenodeoxycholate/taurochenodeoxycholic acid, taurocholate/taurocholic acid (bile acid metabolism pathway members), free fatty acids and carnitines were increased in the AD cohort with higher reported IgE levels, revealing potential energy metabolism disruptions [61], which is in line with our findings. Furthermore, hydroxyl octadecadienoic acids, most of the hydroxy eicosatetraenoic acids (belonging to polyunsaturated fatty acids pathway), as well as glycocholate/glycocholic acid (belonging to bile acid metabolism pathways), were shown to be increased in AD versus healthy controls, independently of patient serum IgE levels (e.g. in cohorts of AD patients with both high or normal levels of serum IgE) [61]. Other studies proposed that the suppression of fatty acids beta-oxidation occurred in mice with AD [62], and mitochondrial dysfunction tended to decrease fatty acid oxidation

and to be associated with higher serum levels of IgE [63].

The complex AD etiopathogenesis is characterized by specific microbiome patterns. The decreased diversity of microbial species with enhanced colonization of staphylococcal species, Staphylococcus aureus (S. aureus) and Staphylococcus epidermidis (S. epidermidis) in particular, is present in AD skin due to inflammation, disrupted skin barrier and reduced levels of antimicrobial peptides [64]. Recent findings demonstrated that overabundant S. epidermidis colonisation, which was previously believed to be beneficial, may have a damaging effect on the skin barrier [65]. Few studies also proposed that gut microbiome disturbances could be related to altered host immune function in AD [3].

Some of the limitations of this study include the lack of experimental validation (for example, quantitative polymerase chain reaction (qPCR) experiments for the identified hub genes) of our findings and the inclusion of a relatively low quantity of AD patient samples. Furthermore, the GEO datasets analysed were classified as AD skin versus healthy skin, with no differentiation between lesional AD and non-lesional AD skin samples, as well as high and normal IgE patient serum levels.

Conclusions

Using the multi-omics approach over AD patient samples datasets, we have identified several novel associations between genes regulating the cell cycle and cell proliferation. Further qRT-PCR validation studies are required to gain additional insights into the role of the identified hub genes in AD pathogenesis.

Acknowledgements

The authors acknowledge support from the NIHR Birmingham ECMC, NIHR Birmingham SRMRC, Nanocommons H2020-EU (731032) and the NIHR Birmingham Biomedical Research Centre and the MRC Health Data Research UK (HDRUK/CFC/01), an initiative funded by UK Research and Innovation, Department of Health and Social Care (England) and the devolved administrations, and leading medical research charities. The views expressed in this publication are those of the authors and not necessarily those of the NHS, the National Institute for Health Research, the Medical Research Council or the Department of Health.

Disclosure of conflict of interest

None.

Abbreviations

AD, Atopic Dermatitis; ASD, Autism Spectrum Disorder; BH, Benjamini-Hochberg; DEGs, Differential expression genes; EN, Elastic Net; GEO, Gene expression data; LASSO, Least absolute shrinkage and selection operator; IMPaLA, Integrated Molecular Pathway-Level Analysis; PPI, protein-protein interactions; miRNA, MicroRNA; qPCR, Quantitative polymerase chain reaction.

Address correspondence to: Dr. Animesh Acharjee, College of Medical and Dental Sciences, Institute of Cancer and Genomic Sciences, University of Birmingham, Edgbaston, Birmingham B15 2TT, UK. Tel: +44-07403642022; E-mail: a.acharjee@bham.ac.uk

References

[1] Tsakok T, Woolf R, Smith CH, Weidinger S and Flohr C. Atopic dermatitis: the skin barrier and beyond. Br J Dermatol 2019; 180: 464-474.

[2] Langan SM, Irvine AD and Weidinger S. Atopic dermatitis. Lancet 2020; 396: 345-360.

[3] Ghosh D, Bernstein JA, Khurana Hershey GK, Rothenberg ME and Mersha TB. Leveraging multilayered "omics" data for atopic dermatitis: a road map to precision medicine. Front Immunol 2018; 9: 2727.

[4] Tsoi LC, Rodriguez E, Degenhardt F, Baurecht H, Wehkamp U, Volks N, Szymczak S, Swindell WR, Sarkar MK, Raja K, Shao S, Patrick M, Gao Y, Uppala R, Perez White BE, Getsios S, Harms PW, Maverakis E, Elder JT, Franke A, Gudjonsson JE and Weidinger S. Atopic dermatitis is an IL-13-dominant disease with greater molecular heterogeneity compared to psoriasis. J Invest Dermatol 2019; 139: 1480-1489.

[5] Tsoi LC, Rodriguez E, Stölzl D, Wehkamp U, Sun J, Gerdes S, Sarkar MK, Hübenthal M, Zeng C, Uppala R, Xing X, Thielking F, Billi AC, Swindell WR, Shefler A, Chen J, Patrick MT, Harms PW, Kahlenberg JM, Perez White BE, Maverakis E, Gudjonsson JE and Weidinger S. Progression of acute-to-chronic atopic dermatitis is associated with quantitative rather than qualitative changes in cytokine responses. J Allergy Clin Immunol 2020; 145: 1406-1415.

[6] He H, Suryawanshi H, Morozov P, Gay-Mimbrera J, Del Duca E, Kim HJ, Kameyama N, Estrada Y, Der E, Krueger JG, Ruano J, Tuschl T and Guttman-Yassky E. Single-cell transcriptome analysis of human skin identifies novel fibroblast subpopulation and enrichment of immune subsets in atopic dermatitis. J Allergy Clin Immunol 2020; 145: 1615-1628.

[7] Jacob M, Gu X, Luo X, Al-Mousa H, Arnaout R, Al-Saud B, L Lopata A, Li L, Dasouki M and Rahman AMA. Metabolomics distinguishes DOCK8 deficiency from atopic dermatitis: towards a biomarker discovery. Metabolites 2019; 9: 274.

[8] Schjødt MS, Gürdeniz G and Chawes B. The metabolomics of childhood atopic diseases: a comprehensive pathway-specific review. Metabolites 2020; 10: 511.

[9] Pavel AB, Zhou L, Diaz A, Ungar B, Dan J, He H, Estrada YD, Xu H, Fernandes M, Renert-Yuval Y, Krueger JG and Guttman-Yassky E. The proteomic skin profile of moderate-to-severe atopic dermatitis patients shows an inflammatory signature. J Am Acad Dermatol 2020; 82: 690-699.

[10] Yin SJ, Cho IH, Yang HS, Park YD and Yang JM. Analysis of the peptides detected in atopic dermatitis and various inflammatory diseases patients-derived sera. Int J Biol Macromol 2018; 106: 1052-1061.

[11] Bieber T, D'Erme AM, Akdis CA, Traidl-Hoffmann C, Lauener R, Schäppi G and Schmid-Grendelmeier P. Clinical phenotypes and endophenotypes of atopic dermatitis: where are we, and where should we go? J Allergy Clin Immunol 2017; 139: S58-S64.

[12] Töröcsik D, Weise C, Gericke J, Szegedi A, Lucas R, Mihaly J, Worm M and Rühl R. Transcriptomic and lipidomic profiling of eicosanoid/docosanoid signalling in affected and non-affected skin of human atopic dermatitis patients. Exp Dermatol 2019; 28: 177-189.

[13] Rojahn TB, Vorstandlechner V, Krausgruber T, Bauer WM, Alkon N, Bangert C, Thaler FM, Sadeghyar F, Fortelny N, Gernedl V, Rindler K, Elbe-Bürger A, Bock C, Mildner M and Brunner PM. Single-cell transcriptomics combined with interstitial fluid proteomics defines cell type-specific immune regulation in atopic dermatitis. J Allergy Clin Immunol 2020; 146: 1056-1069.

[14] Rodríguez E, Baurecht H, Wahn AF, Kretschmer A, Hotze M, Zeilinger S, Klopp N, Illig T, Schramm K, Prokisch H, Kühnel B, Gieger C, Harder J, Cifuentes L, Novak N and Weidinger S. An integrated epigenetic and transcriptomic analysis reveals distinct tissue-specific patterns of DNA methylation associated with atopic dermatitis. J Invest Dermatol 2014; 134: 1873-1883.

[15] Ta LDH, Chan JCY, Yap GC, Purbojati RW, Drautz-Moses DI, Koh YM, Tay CJX, Huang CH, Kioh DYQ, Woon JY, Tham EH, Loo EXL, Shek LPC, Karnani N, Goh A, Van Bever HPS, Teoh OH, Chan YH, Lay C, Knol J, Yap F, Tan KH, Chong YS, Godfrey KM, Kjelleberg S, Schuster SC, Chan ECY and Lee BW. A compromised developmental trajectory of the infant gut microbiome and metabolome in atopic eczema. Gut Microbes 2020; 12: 1-22.

[16] Home-GEO-NCBI. https://www.ncbi.nlm.nih.gov/gds/?term=.

[17] Metabolomics Workbench: Home. https://www.metabolomicsworkbench.org/

[18] GEO2R-GEO-NCBI. https://www.ncbi.nlm.nih.gov/geo/geo2r/.

[19] Ritchie ME, Phipson B, Wu D, Hu Y, Law CW, Shi W and Smyth GK. limma powers differential expression analyses for RNA-sequencing and microarray studies. Nucleic Acids Res 2015; 43: e47.

[20] Gittler JK, Shemer A, Suárez-Fariñas M, Fuentes-Duculan J, Gulewicz KJ, Wang CQF, Mitsui H, Cardinale I, de Guzman Strong C, Krueger JG and Guttman-Yassky E. Progressive activation of T(H)2/T(H)22 cytokines and selective epidermal proteins characterizes acute and chronic atopic dermatitis. J Allergy Clin Immunol 2012; 130: 1344-1354.

[21] Guttman-Yassky E, Suárez-Fariñas M, Chiricozzi A, Nograles KE, Shemer A, Fuentes-Duculan J, Cardinale I, Lin P, Bergman R, Bowcock AM and Krueger JG. Broad defects in epidermal cornification in atopic dermatitis identified through genomic analysis. J Allergy Clin Immunol 2009; 124: 1235-1244, e58.

[22] Mobini R, Andersson BA, Erjefält J, Hahn-Zoric M, Langston MA, Perkins AD, Cardell LO and Benson M. A module-based analytical strategy to identify novel disease-associated genes shows an inhibitory role for interleukin 7 Receptor in allergic inflammation. BMC Syst Biol 2009; 3: 19.

[23] Suárez-Fariñas M, Tintle SJ, Shemer A, Chiricozzi A, Nograles K, Cardinale I, Duan S, Bowcock AM, Krueger JG and Guttman-Yassky E. Nonlesional atopic dermatitis skin is characterized by broad terminal differentiation defects and variable immune abnormalities. J Allergy Clin Immunol 2011; 127: 954-964, e1-4.

[24] Zhou G and Xia J. Using OmicsNet for network integration and 3D visualization. Curr Protoc Bioinformatics 2019; 65: e69.

[25] Tibshirani R. Regression shrinkage and selection via the lasso. Journal of the Royal Statistical Society Series B (Methodological) 1996; 58: 267-288.

[26] Zou H and Hastie T. Regularization and variable selection via the elastic net. Journal of the

Royal Statistical Society: Series B (Statistical Methodology) 2005; 67: 301-320.
[27] Kamburov A, Cavill R, Ebbels TM, Herwig R and Keun HC. Integrated pathway-level analysis of transcriptomics and metabolomics data with IMPaLA. Bioinformatics 2011; 27: 2917-2918.
[28] Zhou G, Soufan O, Ewald J, Hancock REW, Basu N and Xia J. NetworkAnalyst 3.0: a visual analytics platform for comprehensive gene expression profiling and meta-analysis. Nucleic Acids Res 2019; 47: W234-W241.
[29] R: The R Project for Statistical Computing. https://www.r-project.org/.
[30] IntAct Molecular Interaction Database. https://www.ebi.ac.uk/intact/home.
[31] Srivastava N, Gochhait S, Gupta P and Bamezai RN. Copy number alterations of the H2AFX gene in sporadic breast cancer patients. Cancer Genet Cytogenet 2008; 180: 121-128.
[32] Economopoulou M, Langer HF, Celeste A, Orlova VV, Choi EY, Ma M, Vassilopoulos A, Callen E, Deng C, Bassing CH, Boehm M, Nussenzweig A and Chavakis T. Histone H2AX is integral to hypoxia-driven neovascularization. Nat Med 2009; 15: 553-558.
[33] Qiu YT, Wang WJ, Zhang B, Mei LL and Shi ZZ. MCM7 amplification and overexpression promote cell proliferation, colony formation and migration in esophageal squamous cell carcinoma by activating the AKT1/mTOR signaling pathway. Oncol Rep 2017; 37: 3590-3596.
[34] Lau KM, Chan QK, Pang JC, Li KK, Yeung WW, Chung NY, Lui PC, Tam YS, Li HM, Zhou L, Wang Y, Mao Y and Ng HK. Minichromosome maintenance proteins 2, 3 and 7 in medulloblastoma: overexpression and involvement in regulation of cell migration and invasion. Oncogene 2010; 29: 5475-5489.
[35] Marnerides A, Vassilakopoulos TP, Boltetsou E, Levidou G, Angelopoulou MK, Thymara I, Kyrtsonis MC, Pappi V, Tsopra O, Panayiotidis P, Pangalis GA, Beris P, Patsouris E and Korkolopoulou P. Immunohistochemical expression and prognostic significance of CCND3, MCM2 and MCM7 in Hodgkin lymhoma. Anticancer Res 2011; 31: 3585-3594.
[36] Nishihara K, Shomori K, Fujioka S, Tokuyasu N, Inaba A, Osaki M, Ogawa T and Ito H. Minichromosome maintenance protein 7 in colorectal cancer: implication of prognostic significance. Int J Oncol 2008; 33: 245-251.
[37] Qu K, Wang Z, Fan H, Li J, Liu J, Li P, Liang Z, An H, Jiang Y, Lin Q, Dong X, Liu P and Liu C. MCM7 promotes cancer progression through cyclin D1-dependent signaling and serves as a prognostic marker for patients with hepatocellular carcinoma. Cell Death Dis 2017; 8: e2603.
[38] Ren B, Yu G, Tseng GC, Cieply K, Gavel T, Nelson J, Michalopoulos G, Yu YP and Luo JH. MCM7 amplification and overexpression are associated with prostate cancer progression. Oncogene 2006; 25: 1090-1098.
[39] Jankowska-Konsur A, Kobierzycki C, Reich A, Grzegrzolka J, Maj J and Dziegiel P. Expression of MCM-3 and MCM-7 in primary cutaneous T-cell lymphomas. Anticancer Res 2015; 35: 6017-6026.
[40] Hiraiwa A, Fujita M, Adachi A, Ono H, Nagasaka T, Matsumoto Y, Ohashi M, Tomita Y and Ishibashi M. Specific distribution patterns of hCDC47 expression in cutaneous diseases. J Cutan Pathol 1998; 25: 285-290.
[41] Li T, Zhao J, Yang J, Ma X, Dai Q, Huang H, Wang L and Liu P. A meta-analysis of the association between ESR1 genetic variants and the risk of breast cancer. PLoS One 2016; 11: e0153314.
[42] Howard EW and Yang X. microRNA regulation in estrogen receptor-positive breast cancer and endocrine therapy. Biol Proced Online 2018; 20: 17.
[43] Gao S, Ding B and Lou W. microRNA-dependent modulation of genes contributes to ESR1's effect on ERα positive breast cancer. Front Oncol 2020; 10: 753.
[44] Choudhary S, Pradhan D, Khan NS, Singh H, Thomas G and Jain AK. Decoding psoriasis: integrated bioinformatics approach to understand hub genes and involved pathways. Curr Pharm Des 2020; 26: 3619-3630.
[45] Pellacani C, Bucciarelli E, Renda F, Hayward D, Palena A, Chen J, Bonaccorsi S, Wakefield JG, Gatti M and Somma MP. Splicing factors Sf3A2 and Prp31 have direct roles in mitotic chromosome segregation. Elife 2018; 7: e40325.
[46] Fang C, Li L and Li J. Conditional knockout in mice reveals the critical roles of Ppp2ca in epidermis development. Int J Mol Sci 2016; 17: 756.
[47] O'Shea JJ, Gadina M and Siegel R. 9-Cytokines and cytokine receptors. In: Rich RR, Fleisher TA, Shearer WT, Schroeder HW, Frew AJ, Weyand CM, editors. Clinical immunology (Fourth Edition). London: Elsevier; 2013. pp. 108-135.
[48] Griffin DE. Cytokines and Chemokines. In: Mahy BWJ, Van Regenmortel MHV, editors. Encyclopedia of Virology (Third Edition). Oxford: Academic Press; 2008. pp. 620-624.
[49] Angelini F, Di Matteo G, Balestrero S, Brunetti E, Mancino G, Rossi P and Galli E. Nuclear factor κB activity is increased in peripheral blood mononuclear cells of children affected by atopic and non-atopic eczema. Int J Immunopathol Pharmacol 2007; 20: 59-67.
[50] Ewald DA, Malajian D, Krueger JG, Workman CT, Wang T, Tian S, Litman T, Guttman-Yassky E

and Suárez-Fariñas M. Meta-analysis derived atopic dermatitis (MADAD) transcriptome defines a robust AD signature highlighting the involvement of atherosclerosis and lipid metabolism pathways. BMC Med Genomics 2015; 8: 60.

[51] Ghosh D, Ding L, Sivaprasad U, Geh E, Biagini Myers J, Bernstein JA, Khurana Hershey GK and Mersha TB. Multiple transcriptome data analysis reveals biologically relevant atopic dermatitis signature genes and pathways. PLoS One 2015; 10: e0144316.

[52] Hernández-Rodríguez RT and Amezcua-Guerra LM. The potential role of microRNAs as biomarkers in atopic dermatitis: a systematic review. Eur Rev Med Pharmacol Sci 2020; 24: 11804-11809.

[53] Yu X, Wang M, Li L, Zhang L, Chan MTV and Wu WKK. MicroRNAs in atopic dermatitis: a systematic review. J Cell Mol Med 2020; 24: 5966-5972.

[54] Nousbeck J, McAleer MA, Hurault G, Kenny E, Harte K, Kezic S, Tanaka RJ and Irvine AD. MicroRNA analysis of childhood atopic dermatitis reveals a role for miR-451a. Br J Dermatol 2020; 184: 514-523.

[55] Ma L, Xue HB, Wang F, Shu CM and Zhang JH. MicroRNA-155 may be involved in the pathogenesis of atopic dermatitis by modulating the differentiation and function of T helper type 17 (Th17) cells. Clin Exp Immunol 2015; 181: 142-149.

[56] Tonacci A, Bagnato G, Pandolfo G, Billeci L, Sansone F, Conte R and Gangemi S. MicroRNA cross-involvement in autism spectrum disorders and atopic dermatitis: a literature review. J Clin Med 2019; 8: 88.

[57] Longo N, Frigeni M and Pasquali M. Carnitine transport and fatty acid oxidation. Biochim Biophys Acta 2016; 1863: 2422-2435.

[58] van der Veen JN, Kennelly JP, Wan S, Vance JE, Vance DE and Jacobs RL. The critical role of phosphatidylcholine and phosphatidylethanolamine metabolism in health and disease. Biochim Biophys Acta Biomembr 2017; 1859: 1558-1572.

[59] Rivier M, Castiel I, Safonova I, Ailhaud G and Michel S. Peroxisome proliferator-activated receptor-alpha enhances lipid metabolism in a skin equivalent model. J Invest Dermatol 2000; 114: 681-687.

[60] Smith KJ, Dipreta E and Skelton H. Peroxisomes in dermatology. Part II. J Cutan Med Surg 2001; 5: 315-322.

[61] Huang Y, Chen G, Liu X, Shao Y, Gao P, Xin C, Cui Z, Zhao X and Xu G. Serum metabolomics study and eicosanoid analysis of childhood atopic dermatitis based on liquid chromatography-mass spectrometry. J Proteome Res 2014; 13: 5715-5723.

[62] Seino S, Tanaka Y, Honma T, Yanaka M, Sato K, Shinohara N, Ito J, Tsuduki T, Nakagawa K, Miyazawa T and Ikeda I. Atopic dermatitis causes lipid accumulation in the liver of NC/Nga mouse. J Clin Biochem Nutr 2012; 50: 152-157.

[63] Chodaczek G, Bacsi A, Dharajiya N, Sur S, Hazra TK and Boldogh I. Ragweed pollen-mediated IgE-independent release of biogenic amines from mast cells via induction of mitochondrial dysfunction. Mol Immunol 2009; 46: 2505-2514.

[64] Paller AS, Kong HH, Seed P, Naik S, Scharschmidt TC, Gallo RL, Luger T and Irvine AD. The microbiome in patients with atopic dermatitis. J Allergy Clin Immunol 2019; 143: 26-35.

[65] Cau L, Williams MR, Butcher AM, Nakatsuji T, Kavanaugh JS, Cheng JY, Shafiq F, Higbee K, Hata TR, Horswill AR and Gallo RL. Staphylococcus epidermidis protease EcpA can be a deleterious component of the skin microbiome in atopic dermatitis. J Allergy Clin Immunol 2020; 147: 955-966, e16.

[66] https://www.metabolomicsworkbench.org/data/DRCCMetadata.php?ode=Study&StudyID=ST001431.

Supplementary Table 1. Genes with >100 corresponding degrees

GSE36842		GSE6012		GSE16161	
Gene	Degree	Gene	Degree	Gene	Degree
ABARAPL1	519	MYC	769	GRB2	282
MCM7	163	YWHAZ	520	YWHAZ	205
CALM3	148	ARRB2	290	CDC5L	191
PLK1	145	KRT31	280	EGFR	167
HGS	135	TCF4	200	ESR2	141
ZRANB1	124	LIMA1	190	FN1	135
RIF1	123	PIK3R1	181	ESR1	134
UBA1	116	H2AFX	180	TP53	125
MAP3K14	116	UBE2N	176	LNX1	103
GIGYF1	108	MAPK6	173		
		HSPA5	167		
		EEF1A1	156		
		SFN	156		
		CALM3	148		
		EWSR1	147		
		YWHAQ	139		
		TUBB3	126		
		KRT15	119		
		PPP2CA	117		
		SF3A2	116		
		SYNCRIP	113		
		ANXA7	104		
		JUN	103		
		UBE2D3	101		

Supplementary Table 2. List of the 25 most common pathways found within the GSE36842, GSE6012 and GSE16161 datasets

Number	List of the pathways found
1	Class I PI3K signaling events
2	Integrin family cell surface interactions
3	Arf6 trafficking events
4	Endothelins
5	EGF receptor (ErbB1) signaling pathway
6	Beta1 integrin cell surface interactions
7	Plasma membrane estrogen receptor signaling
8	LKB1 signaling events
9	Destabilization of mRNA by AUF1 (hnRNP D0)
10	Ubiquitin-dependent degradation of Cyclin D1
11	CD40/CD40L signaling
12	TNF signaling
13	IRAK2 mediated activation of TAK1 complex
14	Calmodulin induced events
15	TRAF6 mediated induction of NFkB and MAP kinases upon TLR7/8 or 9 activation
16	Nongenotropic Androgen signaling
17	Post-chaperonin tubulin folding pathway
18	PKA activation
19	Ubiquitin-dependent degradation of Cyclin D
20	Endosomal Sorting Complex Required For Transport (ESCRT)
21	PKA-mediated phosphorylation of CREB
22	SCF(Skp2)-mediated degradation of p27/p21
23	Golgi Cisternae Pericentriolar Stack Reorganization
24	Cross-presentation of soluble exogenous antigens (endosomes)
25	SCF-beta-TrCP mediated degradation of Emi1

Supplementary Table 3. miRNA- hub gene interacting pairs

Hub genes and miRNAs	Module
MCM7	1
ESR1	1
hsa-mir-19a-3p	1
hsa-mir-19b-3p	1
hsa-mir-22-3p	1
hsa-mir-26a-5p	1
hsa-mir-100-5p	1
hsa-mir-29b-3p	1
hsa-mir-192-5p	1
hsa-mir-129-5p	1
hsa-mir-1-3p	1
hsa-mir-124-3p	1
hsa-mir-130a-3p	1
hsa-mir-142-3p	1
hsa-mir-145-5p	1
hsa-mir-9-5p	1
hsa-mir-206	1
hsa-mir-302a-3p	1
hsa-mir-301a-3p	1

hsa-mir-130b-3p	1
hsa-mir-302b-3p	1
hsa-mir-302c-3p	1
hsa-mir-302d-3p	1
hsa-mir-372-3p	1
hsa-mir-373-3p	1
hsa-mir-18b-5p	1
hsa-mir-20b-5p	1
hsa-mir-193b-3p	1
hsa-mir-520e	1
hsa-mir-519c-3p	1
hsa-mir-520a-3p	1
hsa-mir-519b-3p	1
hsa-mir-520b	1
hsa-mir-520c-3p	1
hsa-mir-520d-3p	1
hsa-mir-519a-3p	1
hsa-mir-503-5p	1
hsa-mir-583	1
hsa-mir-548d-3p	1
hsa-mir-454-3p	1
hsa-mir-26b-3p	1
hsa-mir-30c-2-3p	1
hsa-mir-30c-1-3p	1
hsa-mir-335-3p	1
hsa-mir-423-5p	1
hsa-mir-874-3p	1
hsa-mir-301b-3p	1
hsa-mir-302e	1
hsa-mir-548p	1
hsa-mir-1910-5p	1
hsa-mir-1914-5p	1
hsa-mir-3184-5p	1
hsa-mir-548x-3p	1
hsa-mir-4295	1
hsa-mir-4268	1
hsa-mir-4264	1
hsa-mir-4290	1
hsa-mir-3666	1
hsa-mir-3668	1
hsa-mir-548z	1
hsa-mir-4422	1
hsa-mir-548ac	1
hsa-mir-548ae-3p	1
hsa-mir-548aj-3p	1
hsa-mir-548am-3p	1
hsa-mir-3121-5p	1
hsa-mir-3157-3p	1
hsa-mir-3944-5p	1
hsa-mir-4671-3p	1

hsa-mir-4709-3p	1
hsa-mir-4797-3p	1
hsa-mir-548ah-3p	1
hsa-mir-548aq-3p	1
hsa-mir-5582-3p	1
hsa-mir-5589-3p	1
hsa-mir-548g-5p	1
hsa-mir-548h-3p	1
hsa-mir-548x-5p	1
hsa-mir-548aj-5p	1
hsa-mir-6073	1
hsa-mir-6085	1
hsa-mir-548e-5p	1
hsa-mir-548j-3p	1
hsa-mir-548f-5p	1
hsa-mir-6757-3p	1
hsa-mir-6788-5p	1
hsa-mir-6813-5p	1
hsa-mir-6871-5p	1
hsa-mir-6878-5p	1
hsa-mir-7852-3p	1
hsa-mir-7855-5p	1
hsa-mir-548bb-3p	1
EEF1A1	2
hsa-mir-16-5p	2
hsa-mir-17-5p	2
hsa-mir-18a-5p	2
hsa-mir-24-3p	2
hsa-mir-25-3p	2
hsa-mir-26b-5p	2
hsa-mir-30a-5p	2
hsa-mir-92a-3p	2
hsa-mir-93-5p	2
hsa-mir-96-5p	2
hsa-mir-30c-5p	2
hsa-mir-221-3p	2
hsa-let-7g-5p	2
hsa-mir-15b-5p	2
hsa-mir-23b-3p	2
hsa-mir-125b-5p	2
hsa-mir-125a-5p	2
hsa-mir-185-5p	2
hsa-mir-186-5p	2
hsa-mir-106b-5p	2
hsa-mir-30e-5p	2
hsa-mir-324-3p	2
hsa-mir-339-5p	2
hsa-mir-423-3p	2
hsa-mir-484	2
hsa-mir-497-5p	2

hsa-mir-501-5p	2
hsa-mir-505-3p	2
hsa-mir-652-3p	2
hsa-mir-421	2
hsa-mir-765	2
hsa-mir-93-3p	2
hsa-mir-296-3p	2
hsa-mir-361-3p	2
hsa-mir-455-3p	2
hsa-mir-877-5p	2
hsa-mir-665	2
hsa-mir-1226-3p	2
hsa-mir-1207-5p	2
hsa-mir-1260b	2
hsa-mir-4328	2
hsa-mir-3150b-3p	2
hsa-mir-4441	2
hsa-mir-4457	2
hsa-mir-4459	2
hsa-mir-4659a-5p	2
hsa-mir-4659b-5p	2
hsa-mir-4731-3p	2
hsa-mir-4736	2
hsa-mir-4763-3p	2
hsa-mir-4776-3p	2
hsa-mir-4784	2
hsa-mir-4801	2
hsa-mir-4482-3p	2
hsa-mir-5590-5p	2
hsa-mir-6499-3p	2
hsa-mir-6840-3p	2
hsa-mir-6888-5p	2
hsa-mir-7150	2
hsa-mir-7159-3p	2
hsa-mir-6516-5p	2
UBA1	3
hsa-let-7b-5p	3
hsa-mir-17-3p	3
hsa-mir-182-5p	3
hsa-mir-210-3p	3
hsa-mir-27b-3p	3
hsa-mir-331-3p	3
hsa-mir-324-5p	3
hsa-mir-615-3p	3
hsa-mir-21-3p	3
hsa-mir-744-5p	3
hsa-mir-1301-3p	3
hsa-mir-1254	3
hsa-mir-1272	3
hsa-mir-3126-5p	3

hsa-mir-4278	3
hsa-mir-4419a	3
hsa-mir-4510	3
hsa-mir-4525	3
hsa-mir-4716-3p	3
hsa-mir-3591-3p	3
hsa-mir-5010-5p	3
hsa-mir-5187-5p	3
hsa-mir-6127	3
hsa-mir-6129	3
hsa-mir-6130	3
hsa-mir-6133	3
hsa-mir-6732-5p	3
hsa-mir-6750-5p	3
hsa-mir-6794-5p	3
hsa-mir-6805-5p	3
hsa-mir-6822-5p	3
hsa-mir-6834-5p	3
hsa-mir-6875-5p	3
PPP2CA	4
hsa-mir-103a-3p	4
hsa-mir-107	4
hsa-mir-197-3p	4
hsa-mir-216a-5p	4
hsa-mir-188-5p	4
hsa-mir-340-3p	4
hsa-mir-519c-5p	4
hsa-mir-518f-5p	4
hsa-mir-526a	4
hsa-mir-522-3p	4
hsa-mir-545-3p	4
hsa-mir-553	4
hsa-mir-584-5p	4
hsa-mir-548c-3p	4
hsa-mir-630	4
hsa-mir-671-5p	4
hsa-mir-33a-3p	4
hsa-mir-92a-1-5p	4
hsa-mir-96-3p	4
hsa-mir-218-2-3p	4
hsa-mir-185-3p	4
hsa-mir-186-3p	4
hsa-mir-889-3p	4
hsa-mir-523-5p	4
hsa-mir-518e-5p	4
hsa-mir-522-5p	4
hsa-mir-519a-5p	4
hsa-mir-519b-5p	4
hsa-mir-520c-5p	4
hsa-mir-518d-5p	4

hsa-mir-513c-5p	4
hsa-mir-548g-3p	4
hsa-mir-224-3p	4
hsa-mir-670-5p	4
hsa-mir-3133	4
hsa-mir-548u	4
hsa-mir-3152-3p	4
hsa-mir-514b-5p	4
hsa-mir-4305	4
hsa-mir-4319	4
hsa-mir-4283	4
hsa-mir-3646	4
hsa-mir-3675-5p	4
hsa-mir-4489	4
hsa-mir-4517	4
hsa-mir-4656	4
hsa-mir-4670-3p	4
hsa-mir-4694-3p	4
hsa-mir-4732-3p	4
hsa-mir-4766-3p	4
hsa-mir-4777-5p	4
hsa-mir-5186	4
hsa-mir-548as-3p	4
hsa-mir-5583-3p	4
hsa-mir-5584-5p	4
hsa-mir-548av-3p	4
hsa-mir-345-3p	4
hsa-mir-758-5p	4
hsa-mir-6079	4
hsa-mir-153-5p	4
hsa-mir-6828-5p	4
hsa-mir-6866-3p	4
hsa-mir-6869-5p	4
hsa-mir-7161-5p	4
hsa-mir-7705	4
hsa-mir-8081	4
hsa-mir-8087	4
hsa-mir-9500	4
TP53	5
hsa-mir-15a-5p	5
hsa-mir-20a-5p	5
hsa-mir-27a-3p	5
hsa-mir-28-5p	5
hsa-mir-106a-5p	5
hsa-mir-30d-5p	5
hsa-mir-10b-5p	5
hsa-mir-34a-5p	5
hsa-mir-214-3p	5
hsa-mir-222-3p	5
hsa-mir-223-3p	5

hsa-mir-30b-5p	5
hsa-mir-150-5p	5
hsa-mir-200a-3p	5
hsa-mir-375	5
hsa-mir-377-3p	5
hsa-mir-330-3p	5
hsa-mir-485-5p	5
hsa-mir-491-5p	5
hsa-mir-518c-3p	5
hsa-mir-504-5p	5
hsa-mir-605-5p	5
hsa-mir-608	5
hsa-mir-612	5
hsa-mir-622	5
hsa-mir-638	5
hsa-mir-663a	5
hsa-mir-26a-1-3p	5
hsa-mir-28-3p	5
hsa-mir-92a-2-5p	5
hsa-mir-214-5p	5
hsa-mir-125b-1-3p	5
hsa-mir-149-3p	5
hsa-mir-150-3p	5
hsa-mir-155-3p	5
hsa-mir-194-3p	5
hsa-mir-151a-5p	5
hsa-mir-505-5p	5
hsa-mir-300	5
hsa-mir-1225-3p	5
hsa-mir-1228-3p	5
hsa-mir-1264	5
hsa-mir-1285-3p	5
hsa-mir-1909-3p	5
hsa-mir-1972	5
hsa-mir-2110	5
hsa-mir-3165	5
hsa-mir-3065-5p	5
hsa-mir-4306	5
hsa-mir-4271	5
hsa-mir-4276	5
hsa-mir-4286	5
hsa-mir-4434	5
hsa-mir-4516	5
hsa-mir-4531	5
hsa-mir-4644	5
hsa-mir-4650-5p	5
hsa-mir-4651	5
hsa-mir-4682	5
hsa-mir-4697-3p	5
hsa-mir-4725-3p	5

hsa-mir-4728-5p	5
hsa-mir-4795-5p	5
hsa-mir-1273f	5
hsa-mir-5003-5p	5
hsa-mir-5193	5
hsa-mir-5196-3p	5
hsa-mir-5197-5p	5
hsa-mir-5587-3p	5
hsa-mir-5693	5
hsa-mir-5702	5
hsa-mir-5703	5
hsa-mir-660-3p	5
hsa-mir-1247-3p	5
hsa-mir-3529-3p	5
hsa-mir-937-5p	5
hsa-mir-1233-5p	5
hsa-mir-6722-3p	5
hsa-mir-1296-3p	5
hsa-mir-513b-3p	5
hsa-mir-6731-5p	5
hsa-mir-6749-3p	5
hsa-mir-6751-5p	5
hsa-mir-6752-5p	5
hsa-mir-6756-5p	5
hsa-mir-6760-5p	5
hsa-mir-6766-5p	5
hsa-mir-6778-5p	5
hsa-mir-6785-5p	5
hsa-mir-6797-5p	5
hsa-mir-6803-5p	5
hsa-mir-6825-5p	5
hsa-mir-6835-5p	5
hsa-mir-6780b-5p	5
hsa-mir-6842-5p	5
hsa-mir-6880-5p	5
hsa-mir-6882-5p	5
hsa-mir-6883-5p	5
hsa-mir-7110-5p	5
hsa-mir-8071	5
hsa-mir-8085	5
hsa-mir-1249-5p	5
GIGYF2	6
hsa-mir-515-5p	6
hsa-mir-519e-5p	6
hsa-mir-454-5p	6
hsa-mir-125b-2-3p	6
hsa-mir-513b-5p	6
hsa-mir-3667-5p	6
hsa-mir-5695	6
hsa-mir-519d-5p	6
hsa-mir-5189-3p	6